Environmental Science: Atmospheres

ROYAL SOCIETY OF CHEMISTRY

PAPER

View Article Online
View Journal

Cite this: DOI: 10.1039/d5ea00115c

Reactive chlorine in the polluted marine boundary layer during the Halifax fog and air quality study (HaliFAQS)

Teles C. Furlani,†[a] Emma M. McLay,[a] Alexander Moravek,‡[a] Cameron E. N. Power,[bc] Aldona Wiacek,[bc] Rachel Y.-W. Chang,[d] Trevor C. VandenBoer *[a] and Cora J. Young *[a]

Chlorine atom (Cl) initiated oxidation of volatile organic compounds (VOCs) yields hydrogen chloride (HCl) that can be detected using a high time-resolution cavity ringdown spectrometer (CRDS). We present continuous HCl measurements in the polluted marine boundary layer during the Halifax Fog and Air Quality Study (HaliFAQS) and demonstrate the efficacy of high time resolution measurements as capable of tracing photochemical Cl formation. Throughout the campaign HCl accumulated at a faster rate alongside high irradiance, particularly in the early morning. Bimodal HCl features were observed on the high irradiance days, consistent with two known photochemical processes: (1) morning photolysis of Cl precursors, and (2) midday photochemical nitric acid (HNO_3) displacing HCl from chloride (Cl^-) containing aerosols. Morning HCl rates of increase and irradiance were used to estimate nitryl chloride ($ClNO_2$) equivalents present at sunrise. We modeled HCl for eight additional, individual days from the campaign based on this estimated $ClNO_2$. The modelled HCl agrees well for six high irradiance days. It captures the features of the morning mode within the combined uncertainty of the estimated $ClNO_2$ and a range of dry deposition rates from the literature. Production of Cl from $ClNO_2$ photolysis ($P(Cl)_{ClNO_2}$) to the production of hydroxyl radical (OH) from the photolysis of measured ozone ($P(HO_x)_{O_3}$) was compared and $P(Cl)_{ClNO_2}$ was found to be 13% of $P(HO_x)_{O_3}$ when considering the full day, and 37% in the morning. Highly time resolved HCl observations can therefore be used to estimate nighttime $ClNO_2$ equivalents and its influence on Cl morning tropospheric oxidation chemistry in polluted coastal atmospheres.

Received 15th September 2025
Accepted 6th January 2026

DOI: 10.1039/d5ea00115c

rsc.li/esatmospheres

Environmental significance

Direct measurements of chlorine atoms do not exist despite their importance to atmospheric oxidation chemistry that regulates air quality and the fate of pollutants. Measurements of molecules that are rapidly destroyed by sunlight to yield a chlorine atom require sophisticated instrumentation run by highly trained personnel. Simple high time resolution techniques that can provide estimates of chlorine atoms and their precursors, such as that for hydrochloric acid by cavity ringdown spectrophotometry, can provide a potential alternative. Field observations in Halifax, Canada found that this technique was capable of such an estimate. We found the chlorine atom contributing a third of measured radical sources in the morning, as has been reported for other polluted coastal atmospheres with more sophisticated instrumentation.

1 Introduction

Tropospheric chlorine (Cl) chemistry influences the fate of atmospheric chemicals, including ozone (O_3), methane, and volatile organic compounds (VOCs).[1,2] Atomic Cl reacts rapidly with VOCs and can contribute to poor air quality through enhancement of the formation of ozone and other secondary atmospheric pollutants by increasing and altering the chemistry of atmospheric oxidation.[3,4] Despite the potential importance of Cl to atmospheric chemistry, many uncertainties remain and many air quality models omit chlorine and other halogen chemistry leading to less accurate modelling.[5] As there

[a]Department of Chemistry, York University, Toronto, Canada. E-mail: tvandenb@yorku.ca; youngcj@yorku.ca
[b]Department of Environmental Science, Saint Mary's University, Halifax, Canada
[c]Department of Astronomy and Physics, Saint Mary's University, Halifax, Canada
[d]Department of Physics and Atmospheric Science, Dalhousie University, Halifax, Canada
† Now at Ministry of Environment, Conservation, and Parks, Toronto, Canada.
‡ Now at German Environment Agency, Department of Air Quality, Dessau-Rosslau, Germany.

are no methods currently able to measure ambient Cl, levels are commonly inferred through models that monitor major sinks (*e.g.*, methane loss *via* (R1), wherein R is CH_3).[6–8] or through measurements of precursors. Several compounds can undergo common photochemical reactions to yield a Cl atom (*e.g.*, HCl, Cl_2, HOCl, ClO, NCl_3 and $ClNO_2$) and are collectively known as Cl_y. Studies to date (*e.g.*, ref. 7–12) have shown the dominant sources of Cl are photolysis of $ClNO_2$ (R2), Cl_2 (R3), trichloramine (NCl_3, (R4)), hypochlorous acid (HOCl, (R5)), reaction of HCl with hydroxyl radicals (OH, (R6)), as well as photocatalytic release from mineral dust-sea spray aerosol containing iron(III) chloride complexes.

$$Cl + RH \rightarrow HCl + R \quad (R1)$$

$$ClNO_2 + h\nu \rightarrow Cl + NO_2 \quad (R2)$$

$$Cl_2 + h\nu \rightarrow 2Cl \quad (R3)$$

$$NCl_3 + h\nu \rightarrow Cl + NCl_2 \quad (R4)$$

$$HOCl + h\nu \rightarrow Cl + OH \quad (R5)$$

$$HCl + OH \rightarrow Cl + H_2O \quad (R6)$$

In the marine boundary layer, the dominant Cl_y processes that dictate Cl atom production in the morning and afternoon are $ClNO_2$ photolysis (R2) and HCl reaction with OH (R6), respectively.[7,8] Formation of $ClNO_2$ occurs primarily at night because the dominant formation mechanism ((R7) and (R8)) requires reaction of a highly photolabile species (*i.e.*, NO_3) that does not exist at appreciable levels during the day.[8,13–19] This, combined with the photolability of $ClNO_2$ itself, limits its importance in most locations globally to Cl production in the morning. The importance of formation of Cl through reaction of HCl typically tracks the abundance of OH, which maximizes near solar noon. For example, along the Santa Monica Bay of Los Angeles, Riedel *et al.* found that $ClNO_2$ photolysis and reaction of HCl each accounted for 45% of the integrated Cl atom production over the entire day, with their maximum contributions occurring at approximately 09:00 and 13:00 local time, respectively.[8]

$$NO_3 + NO_2 \rightleftharpoons N_2O_5 \quad (R7)$$

$$N_2O_{5(g)} + Cl_{(aq)}^- + H_{(aq)}^+ \rightarrow ClNO_{2(g)} + HNO_{3(aq)} \quad (R8)$$

Once formed, the dominant fate of Cl is abstraction of a hydrogen from a VOC (RH) to form HCl (R1).[7] Thus, it is possible that high time resolution HCl measurements could be used to track reaction (R1) and act as a proxy for Cl concentrations. This approach would be reasonably expected to be complicated by direct emissions or other secondary chemical sources of HCl, which include mobilization of chloride (Cl^-) from sea spray aerosol (SSA) through acid displacement ((R9), where M is a cation and HX is a strong acid).[20–25]

$$HX_{(g)} + MCl_{(s\ or\ aq)} \rightarrow MX_{(s\ or\ aq)} + HCl_{(g)} \quad (R9)$$

The most common acid and salt combination for HCl acid displacement are nitric acid (HNO_3) and sodium chloride (NaCl, found in SSA), particularly in marine and coastal atmospheres.[26,27] The rate of acid displacement in the marine boundary layer is typically limited by HNO_3, for which the dominant source is the termolecular reaction between NO_2 and OH, mediated by a third body (M, (R10)). Therefore, the production of HNO_3 is greatest when OH is highest and NO_2 is abundant, which is typically midafternoon in moderately polluted environments.[28–31] Thus, the HCl accumulation rate from this pathway should maximize around the same time.

$$OH + NO_2 + M \rightarrow HNO_3 + M \quad (R10)$$

Thus, there is a temporal separation between the two major sources of HCl, with photolysis of $ClNO_2$ occurring within a few hours after sunrise, and acid displacement following shortly after the solar maximum. Thus, it could be possible to distinguish the two mechanisms using sensitive, high time resolution HCl measurements.

Tropospheric HCl levels commonly range from 10 to 1000 parts per trillion by volume (pptv).[32–35] *In situ* high-time response measurements are challenging due to the fact HCl is a surface-active gas that readily sorbs to inlet materials.[34,36] Online measurements on the order of seconds to minutes have been generally accomplished by chemical ionization mass spectrometry (CIMS),[34,37–39] but emerging spectroscopy-based techniques have been shown to have desirable qualities for field deployment, including high accuracy, atmospherically-relevant detection limits, simple operation, and portability.[32,36,40–42] *In situ* high time-response measurements provide more information on HCl sources and sinks when compared to traditionally-used methods which rely on time integrated (2 hours – days) scrubbing of ambient air followed by offline analysis.[26,33] Marine boundary layer observations with high time response instruments have indicated that Cl activation chemistry to produce $ClNO_2$ is promoted in coastal urban locations, yet this chemistry has rarely been explored in a Canadian context, despite having several highly active ports and an extensive coastline. Observations of low levels of $ClNO_2$ ~35 km from the Pacific Ocean in Abbotsford, British Columbia suggested that production was restricted to the nocturnal residual layer as insufficient O_3 for NO_3 formation was available in the nocturnal boundary layer.[43] In contrast, observations of NO_2 and NO_3 from Saturna Island suggested that $ClNO_2$ activation over the Salish Sea within the nocturnal boundary layer could proceed readily.[44] In the latter study, enhancements in O_3 production in transported air masses were identified as a potential consequence of this Cl activation chemistry.

In this study we measured HCl at high time resolution with a cavity ringdown spectrometer in late spring/early summer in the Canadian coastal city Halifax, which is home to a highly active port, for the Fog and Air Quality Study (HaliFAQS). Supporting measurements of other ambient pollutants (*e.g.*, O_3, NO_x, formaldehyde) were used to explore the potential role of Cl activation chemistry and it impacts on atmospheric oxidation processes. We identified HCl formation mechanisms; inferred

the contribution of $ClNO_2$ photolysis to Cl formation; and compared the estimated Cl atom source to other radical sources to situate the utility of this technique and compare the potential role of Cl to other coastal urban locations around the world.

2 Methods

2.1 HaliFAQS campaign

Sampling was conducted as part of the HaliFAQS ground based atmospheric chemistry field campaign in Halifax, Nova Scotia, Canada (population ~400 000) from May 25 to June 25, 2019. All measurements were made from the rooftop lab of the five story St Mary's University Student Centre building (44°37′55.8″N, 63° 34′48.4″W, ~50 m above sea level, including building height). The outdoor temperatures ranged from 5 to 25 °C (mean of 13.3 °C) and the RH ranged from 26 to 98% (mean of 76%). The site was predominantly influenced by air masses arriving from the Atlantic Ocean (east) *via* the port entry of Halifax, as shown in Fig. S1. Measured by container volume, the port of Halifax is the fourth largest port in Canada and connected to more than 150 countries *via* 18 direct shipping lanes.[45] The port is integrated into the downtown area of the city and located roughly 1.5 km from the measurement site. Emissions (*e.g.*, NO_x) from this shipping traffic may influence some of the chemistry reported in this study.

2.2 Hydrochloric acid (HCl) measurement

Gaseous HCl was measured at 0.5 Hz using a cavity ring-down spectrometer (CRDS, Picarro G2108). The CRDS measures absorption of the first overtone of HCl at 5739 cm^{-1}. The limit of detection was 18 pptv for a 30 second integration time, and the accuracy of the instrument has been validated by intercomparison.[42] Further details on the application and validation of this instrument for making atmospheric measurements is described in detail in Furlani *et al.*, (2021).[42] All indoor inlet lines and fittings were kept in a thermostated room that fluctuated from 25 to 30 °C. All inlet lines and fittings were made of perfluoroalkoxy alkane (PFA) unless stated otherwise. A full schematic and description of the sampling inlet indicating the separation between the outdoor and indoor inlet line lengths, analyzers, and flows is provided in Section S2 and Fig. S2 of the SI.

2.3 Supporting measurements and variables

Supporting measurements for the HaliFAQS campaign were collocated with the HCl inlet and included NO, NO_x, O_3, formaldehyde (HCHO), solar irradiance, and meteorology (temperature, pressure, relative humidity, wind speed and direction). The NO and NO_x were measured using the chemiluminescence of NO (American EcoTech EC9841), with NO_2 converted to NO with a molybdenum converter for the NO_x measurement and NO_2 determined by difference. The O_3 was measured using UV absorption spectrophotometry (American EcoTech Serinus 10). Gas-phase HCHO (spectral window 2745–2800 cm^{-1}) was measured using open-path Fourier transform infrared spectroscopy (OP-FTIR) with additional details in Section S2.[45] Timeseries for these supporting measurements are provided in Fig. S1 and S3.

Solar irradiance measurements (kW m^{-2}) were captured using a HOBO S-LIB-M003 Solar Radiation Smart Sensor paired with a HOBO H21-USB Micro Station data logger. A Davis Vantage Pro 2 weather station was used to monitor outdoor pressure, temperature, wind speed, and wind direction, with sensors mounted on an ~3 m mast above the rooftop for an overall height of ~28 m above ground level. Planetary boundary layer height was extracted for the campaign period from the Environment and Climate Change Canada (ECCC) High Resolution Deterministic Prediction System (HRDPS) Global Environmental Multiscale (GEM) model (2.5-km resolution) forecast archives (Fig. S4).[46] Photolysis rate coefficients were calculated using the National Center for Atmospheric Research (NCAR) tropospheric ultraviolet and visible (TUV) radiation model-version 5.3.[47]

2.4 Box model for estimating mixing ratios of morning $ClNO_2$ and resulting HCl production

Using our observations and the variable determinations from the prior section, a box model was developed to first estimate the mixing ratio of $ClNO_2$ present from the preceding night, followed by a model determination of the overall contribution $ClNO_2$ could make to the observed HCl. The box model is constrained to this Cl precursor because past studies have shown that the dominant photolabile Cl precursor in North American marine atmospheres is $ClNO_2$ at sunrise, with Cl_2 generally playing a minor role (<10%),[8,38] though recent measurements in Asia have reported the regional importance of Cl_2.[3] The photolysis of $ClNO_2$ leads to the production of Cl (R2), for which the dominant fate is rapid H-abstraction with an organic to form HCl (R1). In Los Angeles, HCl formation was estimated to range from 69–77% of the total Cl reactivity. This conversion efficiency (CE) of Cl to HCl would be expected to be higher in atmospheres with lower quantities of inorganic pollutants (*e.g.*, NO_x).[7,48] Hydrogen abstraction would in turn dominate the production of HCl from Cl, as acid displacement would require substantial production of HNO_3 and therefore require NO_x.

This process would be expected to maximize the rate of HCl production on days with clear-sky irradiance available in the early morning. In such a situation, it is reasonable to assume that HCl mixing ratios accumulated above the pre-dawn baseline originate from (R2) and (R1), while also being continuously deposited to the ground surface within the planetary boundary layer (PBL). That is, we can assume the rate of HCl formation is proportional to the photolysis rate of $ClNO_2$. The change in HCl concentration (ΔHCl) term in (E1) was determined for 15-minute intervals in this campaign, calculated as the deposition-corrected difference between two consecutive measurements (*i.e.* $[HCl']_t - [HCl']_{t-1}$, where [HCl′] is the deposition-corrected mixing ratio). The accumulation of HCl in (E1) then describes the amount originating from the photolysis of $ClNO_2$, when assuming the yield from Cl is 100%.

$$\Delta HCl = j_{ClNO_2}([ClNO_2]_i - \Sigma HCl)\Delta t \quad \text{(E1)}$$

The Δt term is the change in time for each 15-minute interval (equivalent to 900 seconds) and is considered from 04:30 (about

one hour before sunrise) to 10:30, which is the time when we assume $ClNO_2$ has fully photolyzed. All times are 24-h format and presented in Atlantic Daylight Time (ADT). The $[ClNO_2]_i$ represents the mixing ratio of $ClNO_2$ present at sunrise; and ΣHCl is the sum of HCl formed since sunrise (*i.e.* the sum of all ΔHCl values up to the current pair of consecutive measurement intervals in (E1)).

Since HCl is a strong acid, it readily deposits to the ground surface from the PBL like HNO_3, which means the term is necessary to capture in the box model. Deposition was considered for the determinations of both ΔHCl and ΣHCl where we generated two sets of the independent variables that correspond to low (1 cm s^{-1} or 1×10^{-2} m s^{-1}) and high (6 cm s^{-1} or 6×10^{-2} m s^{-1}) deposition velocities. This range is derived from those reported for HCl and HNO_3 in the literature where a range of 1–5 cm s^{-1} is often reported for marine environments.[34,49,50] The topography of the city of Halifax is expected to have a higher surface roughness in comparison to open ocean, so a higher upper limit of the deposition velocity range is reasonable to explore. A 1 cm s^{-1} increase compared to the reported values brings the upper limit of this study to 6 cm s^{-1}, which is consistent with findings for HNO_3 in forested environments.[49] Here, our model encompasses as much of the uncertainty from this parameter as possible to demonstrate the need for more field observations, which are highly limited at present.[51] Then, using the GEM modelled PBL height (h_{PBL}; m) and measured HCl, loss *via* deposition ($L_{HCl,dep}$; molecules m^{-3} s^{-1}) was calculated as the ratio of the deposition velocity (v_{dep}; m s^{-1}) to the PBL height multiplied by the HCl number density (molecules m^{-3}) as in (E2). These range limits are valuable as the deposition velocities of HCl are not certain and heavily dependent on surface roughness and loss mechanisms of HCl at the surface.

$$L_{HCl,dep} = \left(\frac{v_{dep}}{h_{PBL}}\right)[HCl] \quad \text{(E2)}$$

The losses *via* deposition were multiplied by the length of time over which the loss occurred (Δ*t*; s) and the value was added to the HCl measurements ([HCl]; molecules m^{-3}) to obtain a deposition-corrected HCl production expressed as a concentration ([HCl′]; molecules m^{-3}), as in (E3), prior to calculation of the ΔHCl and ΣHCl independent variable sets for (E1).

$$[HCl'] = L_{HCl,dep}\,\Delta t + [HCl] \quad \text{(E3)}$$

Accounting for deposition in the model is expected to reduce bias in the subsequent regression analysis described below. Using the TUV model, photolysis rate coefficients (*e.g.* j_{ClNO_2}) were then calculated under clear-sky conditions, also at 15-minute intervals. The clear-sky *j*-values were scaled to observed irradiance using the ratio of 15-minute measured irradiance to the theoretical maximum clear sky irradiance at each time point (see SI, Section S1).[47,52–54]

We identified study days in which photolabile Cl precursors were likely to be major contributors to observed HCl using the criteria of an early morning with irradiance at or near clear-sky conditions and with a fast accumulation of HCl mixing ratio – tens to hundreds of pptv per hour. We also selected control days that had a low morning irradiance relative to the campaign average and a slow rate of change in HCl. In total, we examined eight days from the observational dataset. The three measurement-derived variables ΔHCl, j_{ClNO_2}, and ΣHCl were then used to determine $[ClNO_2]_i$ for each day. The initial $ClNO_2$ determination was conducted using a least-squares regression analysis with a custom fitting function for (E1) in Igor Pro 8 (Wavemetrics, OR, USA). The best time interval to predict this initial amount across all examined days was subject to a sensitivity analysis (Section S3, Table S1), which evaluated the relative error in the linear fit as the metric to quantify our assumption of linear accumulation (Table S2). This test found that 8:00 to 10:30 ADT was the most robust period to determine the initial $ClNO_2$ used in the model. All model results returned reasonable mixing ratios of $ClNO_2$ present at sunrise (tens to a couple hundred pptv; Tables S1 and S2) and consistent with reports from other North American coastal cities.[8,39,55,56] Meanwhile the entirety of the modeling period simply followed the prescribed HCl production and loss processes. Each day had two calculated $[ClNO_2]_i$ values which could then be used to compare to the observed rate of change in HCl, when being inclusive of the uncertain 1–6 cm s^{-1} deposition loss range.[8,49]

With the calculated initial $ClNO_2$ concentrations and the j_{ClNO_2} values corrected for irradiance, the HCl concentrations can be modelled for each 15-minute time period within a full day, starting from a baseline value. This is achieved through the calculation of the new HCl production at each time step through $ClNO_2$ photolysis after sunrise and the addition of this to any previously formed HCl, that has been corrected for dry deposition loss from both 1 cm s^{-1} and 6 cm s^{-1} velocities. The HCl determination was parsed further for a range of yields from the production of Cl atoms *via* (R1), ranging from 100% (representing a theoretical upper limit) to 77% CE (Section S4, Table S3). Using this model, HCl at a given timepoint ($[HCl]_t$; molecules m^{-3}) can be calculated by adding the accumulated [HCl] at the previous time point ($[HCl]_{t-1}$; molecules m^{-3}) to the newly produced HCl since that time, which is calculated using the photolysis rate constant (j_{ClNO_2}; s^{-1}) of $ClNO_2$, the irradiance correction factor (ICF) for this value, the CE, and the $ClNO_2$ concentration at a given time, and subtracting the loss of HCl that occurred in the intervening time as described by (E2). The HCl concentration at a given time is thus calculated (E4).

$$[HCl]_t = [HCl]_{t-1} + j_{ClNO_2}(ICF)(CE)[ClNO_2]_i\Delta t - \frac{v_{dep}}{h_{PBL}}[HCl]_{t-1}\Delta t \quad \text{(E4)}$$

2.5 Radical production comparison for Cl and HO_x in Halifax

Two days were selected for calculating radical production: June 13 and 18—both of which exhibited good correlation between modelled and measured HCl ($R^2 > 0.85$, Fig. S5). The $[ClNO_2]_i$ corresponding to high and low HCl deposition conditions was calculated and the midpoint of the range for each day was used to calculate Cl production. Photolysis of $[ClNO_2]_i$ was then calculated in 15-minute intervals using the matched temporal

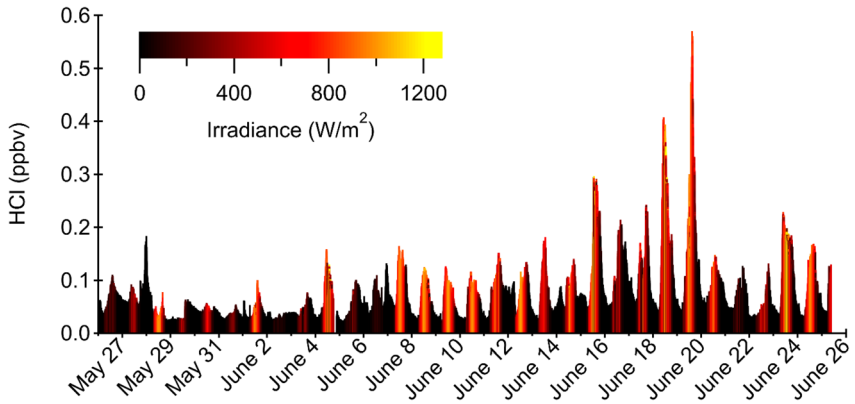

Fig. 1 Mixing ratio timeseries of HCl from May 25 to June 25, 2019, for the HaliFAQS campaign. The colored scale represents colocated irradiance measurements.

irradiance-normalized photolysis rate coefficients from TUV. We assumed no sources of $ClNO_2$ existed after sunrise.

We calculated hydrogen oxide ($HO_x \equiv OH + HO_2$) primary radical production by using surface level measurements of O_3 (R11)–(R13) and HCHO ((R14) and (R15)).

$$O_3 + h\nu \rightarrow O_2 + O(^1D) \quad \text{(R11)}$$

$$O(^1D) + M \rightarrow O(^3P) + M \quad \text{(R12)}$$

$$O(^1D) + H_2O \rightarrow 2OH \quad \text{(R13)}$$

$$HCHO + h\nu \rightarrow H + CHO \quad \text{(R14)}$$

$$H + O_2 + h\nu \rightarrow HO_2 \quad \text{(R15)}$$

Photolysis rate coefficients for O_3 (j_{O_3}) and HCHO (j_{HCHO}) were calculated following the same procedure as described above for j_{ClNO_2}. Ozone measurements for 13 and 18 June were averaged to 15-minute intervals and combined with j_{O_3}, pressure, and RH to calculate the production of OH ($P(HO_x)_{O_3}$). Formaldehyde was diurnally averaged across several similar days that includes the two study days, due to the limited period of observations within the overall campaign. The diurnal HCHO measurements were then averaged also to 15-minute intervals and the reaction of H atoms with molecular oxygen (R15) was assumed to be instantaneous, such that it could be used to determine $P(HO_x)_{HCHO}$.

3 Results and discussion

3.1 HCl measurements and sources

Measurements of HCl during HaliFAQS ranged between a daytime maximum of 572 pptv and a nighttime minimum of 55 pptv, with a 24-h mean value of 97 pptv (Fig. 1). In most instances, HCl levels were higher during the day than at night and were elevated when originating from the southeast (Fig. S6). We typically observed higher HCl on days accompanied by high solar irradiance (Fig. 2 and S7). These trends are generally consistent with the literature (Tables 1 and S4), where HCl formation has been attributed to be a consequence of photochemical processes, either acid displacement by photochemically-generated HNO_3 ((R9) and (R10)) or reaction of photochemically-generated Cl with organics (R1). The HCl levels in Halifax are midrange globally, situated between the higher, more extreme values for locations like Los Angeles, USA and lower values for remote areas like Antarctica (Table 1).

Elevated levels of HCl observed at night most likely result from direct emissions.[32] For example, suspected direct emissions of HCl were observed during the nights of May 27 and June 6 (Fig. 1). Low levels of observed HCl and irradiance from May 26—June 6 were coincident with fog formation events and overall cloudy local conditions. Incidences of light rain during this timeframe could promote wet deposition loss of HCl as well. Temperatures tended to be lower during this period and would be expected to correspond to a less mixed boundary layer, with potential stratification. Such a situation might explain some of the rapid and unpredictable changes (*e.g.*, May 29 at ~14:00) in HCl from horizontal advection or mixing entrainment from aloft.

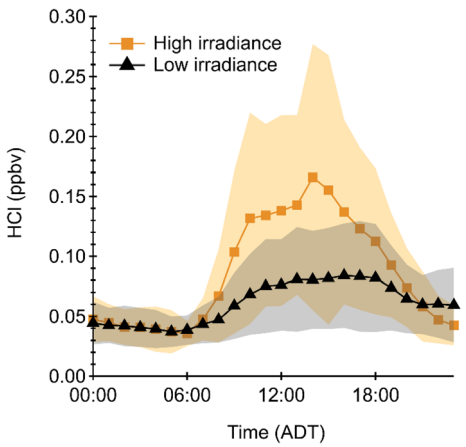

Fig. 2 Diurnally averaged hourly observations of HCl for the full HaliFAQS campaign. Measurements are separated by days with high and low irradiance. See the text for a description of the definition of high and low irradiance days. Shaded areas represent the standard deviation in the hourly HCl measurement.

Table 1 Summary of selected global measurement ranges of HCl mixing ratios in the marine boundary layer reported after December 2000. Numbers in brackets represent the mean campaign values. Where mixing ratios are presented with '<', this indicates the method detection limit. If a detection limit was not reported, the lower limit was given a value of zero

Country	City/region	Date	Method	HCl (pptv)	References
Canada	Halifax, Nova Scotia	May–June 2019	CRDS	55–572 (97)	This study
Canada	St John's, Newfoundland	April 2017	CRDS	<20–1210 (63)	Angelucci *et al.*, (2021)[32]
USA	Northern California coast	February–March 2015	Iodide CI-TOF-MS	100–380 (199)	Haskins *et al.*, (2018)[38]
USA	Southern California coast	February–March 2015	Iodide CI-TOF-MS	530–2700 (1300)	Haskins *et al.*, (2018)[38]
Cyprus	N/A	July–August 2014	Iodide CI-QMS	<135–3000 (790)	Eger *et al.*, (2019)[37]
USA	Central California coast	May–June 2010	Acetate CI-TOF-MS	0–2800 (440)	Crisp *et al.*, (2014)[34]
USA	Southern California coast	May–June 2010	Acetate CI-TOF-MS	0 to > 16 000 (2200)	Crisp *et al.*, (2014)[34]
USA	Pasadena, California & San Joaquin Valley, California	May–June 2010	Acetate CI-TOF-MS & AIM-IC	<55–5950 (830) & <19–776 (84)	Tao *et al.*, (2022)[57]
Cape Verde	Sao Vicente Island	May–June 2007	Tandem Mist Chamber/IC	50–600	Lawler *et al.*, (2009)[58]
USA	Appledore Island, Maine	July–August 2004	Tandem Mist Chamber/IC	5–5800 (600)	Keene *et al.*, (2007)[26]
Germany to South Africa	Eastern North and South Atlantic	October–November 2003	Tandem Mist Chamber/IC	20–1400	Keene *et al.*, (2009)[33]
Antarctica	Dumont d'Urville	December 2000–December 2001	Tandem Mist Chamber/IC	30–300	Jourdain and Legrand, (2002)[59]
USA to Canada	South Carolina coast	July–August 2002	Tandem Mist Chamber/IC	<25–4500	Keene *et al.*, (2004)[60]

Our results are similar to those reported using the same technique in another Atlantic Canadian city (St. John's, Newfoundland and Labrador, ~900 km northeast of Halifax; Table 1) in early spring.[32] The HCl levels for our dataset were higher than those observed in St John's (63 pptv). The greater overall irradiance that occurred during HaliFAQS could be more effective at accessing HCl precursor reservoirs. However, the maximum value observed in St John's (1220 pptv) also coincided with high irradiance and actually exceeded our highest observed value during HaliFAQS, suggesting that reservoir species may have been abundant. The results from both studies suggest a substantial photochemical relationship between precursors and daytime HCl production. To further determine the importance of photochemical processes, we examined diurnal trends sorted by irradiance levels. We defined high irradiance days as those within 25% of the maximum integrated irradiance observed during HaliFAQS, making any remaining days classified as low irradiance (Fig. 2 and S7).

We observed bimodal features in many high irradiance days, with the center of the HCl modes maximizing at 10:00 and 14:00 ADT. On some high-irradiance days, we observed only a single mode corresponding to high HCl in one of either the morning or afternoon periods. The bimodal feature could infer that two photochemical mechanisms previously established as HCl sources are driving its production in the marine boundary layer. The mechanisms are the photolysis of photolabile Cl_y to explain the earlier peak and acid displacement of regional sea spray aerosol Cl^- by HNO_3 for the later peak. Both photochemical mechanisms are important for HCl production and are heavily influenced by NO_x pollution.[32] Fig. S9 illustrates a parameter space wherein the two mechanisms both require high irradiance to enhance HCl mixing ratios, but one also correlates with our estimated production of HNO_3, while the other is independent of it. Thus, the independent mechanism occurs when OH is low, and our estimated production of HNO_3 is small regardless of NO_2 abundance. In such a scenario, the elevated accumulation rate of HCl is likely to be from Cl H-abstraction processes (R1). The HNO_3-dependent mechanism shows a smaller increase in HCl overall, as expected due to the series of reactions required to reach the acid-displacement step of (R9).

These two HCl production pathways rely on many of the same external factors such as irradiance, NO_x and Cl^- containing SSA. Examining the relationship between HCl, time of day, and irradiance, can provide insight into the relative importance of these two pathways. Days with an observed afternoon mode of HCl formation (*e.g.* June 7 and 17) saw a maximum feature occur between 14:00–18:00 ADT, which is consistent with the expected maximum in photochemical production and reactive uptake of HNO_3 for acid displacement on sea salt aerosol, which is ubiquitous in coastal atmospheres. Determining the contribution from these two mechanisms is complex and heavily dependent on the temporal and spatial trends of daily local precursor emissions. We observed that quick-rising HCl in the morning that led to a mid-day maximum

often coincident with elevated irradiance. The relationship between irradiance and HCl in the early morning in 22 of our 31 measurement days suggests photolysis of photolabile precursors as a likely mechanism (Fig. S8). Only one day, May 28, had high morning irradiance and a low rate of accumulation of HCl, which is consistent with limited to no Cl precursor production the previous night and/or it not being available at the surface where our measurement was located throughout the morning hours. Due to the strength of the relationship with irradiance, the formation of HCl from photolysis of photolabile precursors was explored further using our developed box model (Section 2.4).

3.2 A box model to explore HCl formation and assess the contribution of photolabile Cl_y to radical formation

The box model was used to predict HCl mixing ratios at 15-minute time resolution from the photochemical production of Cl atoms, initiated from an estimate of $ClNO_2$ present at sunrise (Fig. 3, and S10–S12). While this approach to modelling HCl does not include other parameters that could affect the HCl mixing ratio, including direct emissions or advection, vertical mixing, and acid displacement there is little evidence of these processes being substantial contributors during the selected days from this campaign. We expect the majority of our HCl observation days to be dominated by acid displacement, as reported in a previous study in coastal Canada.[32] The range of reactivities/conversion efficiencies that was used in this model (77–100%), as introduced in Section 2.4, is an estimate based on a previous study in Los Angeles.[7] Due to the location- and condition-dependent nature of this reactivity, this relatively wide range was chosen to encompass uncertainties in regard to this, and it is reflected in the resulting range of modelled HCl (Fig. 3). Another assumption made is that $ClNO_2$ is the only photolabile Cl precursor that yields HCl and our estimates are in reasonable agreement with the literature (Tables S1 and S2). Attempts to include relevant levels of Cl_2 (1–20 pptv) were found to have a negligible influence on the predicted HCl magnitude and trend. This is consistent with observations of low Cl_2 relative to $ClNO_2$ in other coastal locations.[4,8,56] Therefore, it was not included in the HCl model for Halifax. Simulating and comparing to the measured HCl allows us to evaluate the estimation method as an indirect measure of $ClNO_2$ as the Cl source, but in reality, it represents a combined outcome from all photolabile Cl atom reservoirs and other uncaptured processes represented chemically as $ClNO_2$. Similarly, we know that reservoirs may form aloft and mix to the surface during the morning breakup of the nocturnal boundary layer,[55] which would be captured by our model estimate of morning $ClNO_2$ equivalents. However, our model cannot capture a scenario where HCl produced aloft at night is mixed to the surface.

Predicting the HCl generated from the photolysis of our estimated precursor (see $[ClNO_2]_i$ in (E1)) and comparing it to the measured HCl that originates from all atmospheric processes is used here to illustrate that early morning changes in HCl concentration resemble the trends expected from a photolabile Cl precursor. The sum of photolabile Cl precursors agrees with the temporal increase of the measured HCl in the morning, even when entirely represented by $ClNO_2$ as an assumption in the model. It even has the ability to explain observed HCl beyond the 10:30 AM boundary of the data

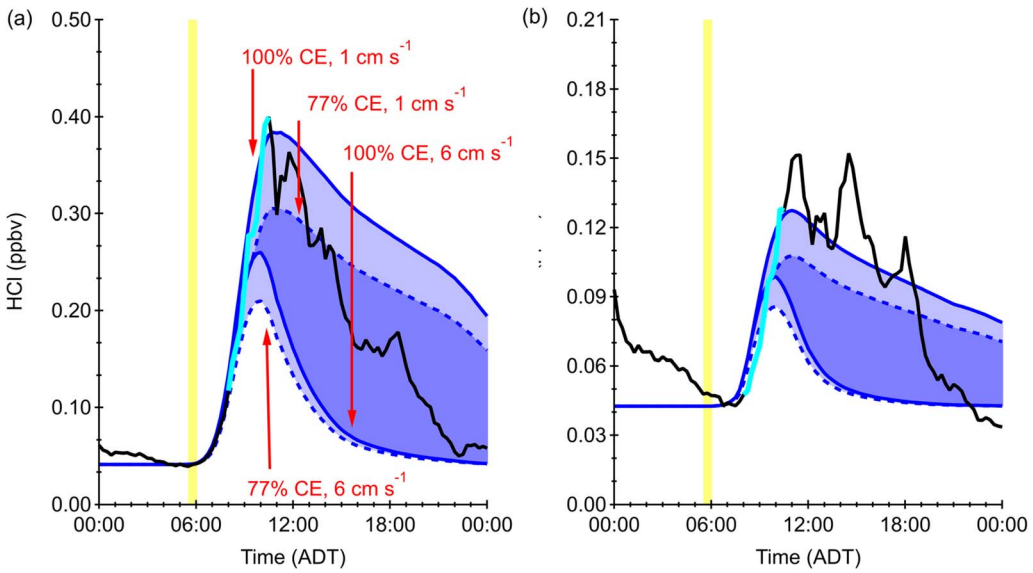

Fig. 3 Measured HCl (black) and modelled HCl (blue) predicted from photolysis of the initial $ClNO_2$ estimated for (a) June 18 (category (i) day) and (b) June 7 (category (ii) day). Blue shading indicates the uncertainty in the modelled HCl from the range of deposition velocities and conversion efficiencies. From top to bottom, the 4 modelled traces are those for 100% CE and 1 cm s^{-1} deposition velocity, 77% CE and 1 cm s^{-1} deposition velocity, 100% CE and 6 cm s^{-1} deposition velocity, and 77% CE and 6 cm s^{-1} deposition velocity. Dotted traces represent 77% CE cases while solid lines indicate the 100% CE cases. The yellow vertical line denotes time at sunrise and the cyan section of the measured HCl trace indicates the period used to estimate the amount of initial $ClNO_2$ present in the first part of the box model. Note that the *y*-axis scales differ between the panels.

initially used to constrain the model (Fig. 3, and S10–S12). Most of our study days show good agreement between predicted and measured HCl throughout the morning and midday. Based on the model-observation comparison shown across Fig. 3, and S10–S12, we can characterize the observed diurnal pattern of HCl as: (i) days with primarily early morning HCl formation; (ii) days with both morning and afternoon formation of HCl; and (iii) days with overlap between these two mechanisms but an overall undistinguishable dominant mechanism.

The days that solely have HCl production in the morning mode (category (i)) were June 13 and 18, with the model-measurement results of the latter depicted in Fig. 3 and the former in Fig. S10; these days had a single early and fast-rising HCl peak that coincided with high irradiance in the early morning. The absence of a strong afternoon peak of HCl on these days is due to low availability of our estimated photochemical HNO_3 which would have driven acid displacement on the abundant regional sea spray aerosol. This is consistent with the observed NO_2 being lower on these days (~5.5 ppbv) compared to ~15 ppbv on days with an observed second mode, as well as the clear separation of HCl mixing ratio from our HNO_3 proxy in many instances (Fig. S9), but not all of them (Fig. S13). In the latter situation, note that our estimated HNO_3 proxy is not quantitative and assumes an excess availability of chloride for displacement reactions. While we do not expect to capture the entirety of the HCl magnitude, variance, or trend with our model, the very close match in all of these metrics between measurement and model data on these days strongly supports our hypothesis that $ClNO_2$ photolysis is driving a substantial amount of the morning through midday production of Cl, and ultimately HCl, in the polluted marine boundary layer of Halifax. Generally, the deposition velocity of 1 cm s^{-1} and Cl to HCl conversion efficiency of 77% produce the most comparable model HCl mixing ratios when they are elevated above the initial baseline. The high deposition velocity model results best capture the return of the HCl mixing ratios to the baseline later in the day. The deposition velocity for this environment appears to lie closer to 1 cm s^{-1} rather than 6 cm s^{-1} from our exploration of this parameter space but may change with local micrometeorology and surface roughness over time, which is beyond the scope of this work. The use of high time resolution HCl measurements that are similar to the timescale of $ClNO_2$ photochemistry, in a location where this precursor is expected to be readily formed, are critical to undertaking further analysis.

The days on which two clear peaks of HCl were observed (category (ii)) were June 7 and 17, with the 7th depicted in Fig. 3 and the 17th in Fig. S11. The predicted HCl agrees with the measurement magnitude and trend early in the day but deviates later in the afternoon and early evening. This suggests that the peak mixing ratio and rate of increase corresponding to the morning mode for HCl was influenced by photolytic formation of Cl, while the production later in the day was likely caused by acid displacement. These bimodal days illustrate that the two competing chemical pathways in daily HCl production are very likely active. For example, the availability of proxy HNO_3 on June 7 is present throughout the day and is elevated an hour or two before peaks in HCl mixing ratios are observed where the Cl-precursor reservoir cannot explain the temporal trend (Fig. S13). This is consistent with the slower timescale of acid displacement chemistry compared to that of radicals.

The days that had an indistinguishable dominant mechanism (category (iii)) were June 3, 5, 15, and 19 (Fig. S12). It is possible that direct emissions or other HCl sources could be influencing HCl levels on these days. June 3 and 5 were days where irradiance was <10% of maximum daily integrated irradiance and had some of the lowest observed levels of HCl (40 and 48 pptv, on average, respectively; Fig. S12). These also had some of the poorest agreement between model and measurement but did result in a good comparison for June 5 despite photochemical mechanisms for either daytime HCl source being strongly suppressed.

Including HCl measurements more routinely at higher time resolution for atmospheric measurements in coastal locations, particularly those that are urban and can activate halogen radical chemistry, could provide a valuable complimentary approach to inferring Cl chemistry along with the additional, more complex and resource-intensive instrumentation, that is currently used most often. Conversely, to study HCl atmospheric chemistry mechanistically, direct measurements of at least NO_x, O_3, NO_3, N_2O_5, $ClNO_2$, Cl_2, NCl_3, and HNO_3, as well as aerosol composition, at high time resolution are ideal to provide a better basis on which to interpret and differentiate direct emissions and the photochemical sources for HCl in the marine boundary layer. This could lead to a better

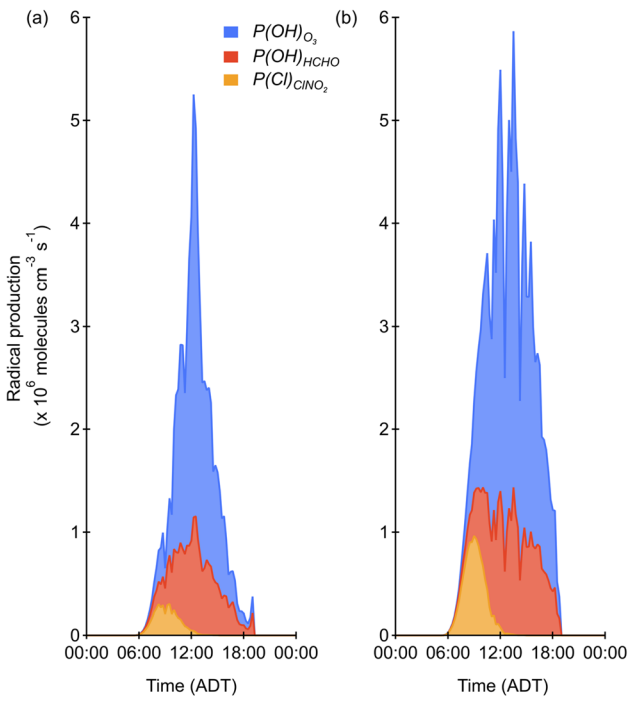

Fig. 4 Comparison of major ground-level radical sources: $P(HO_x)$ from reaction of $O(^1D)$ from O_3 photolysis with water (blue), $P(HO_x)$ from diurnally averaged HCHO photolysis (red-orange), and P(Cl) from predicted $ClNO_2$ photolysis (yellow-orange), for (a) June 13, and (b) June 18. Traces are stacked so the upper limit is the cumulative radical production.

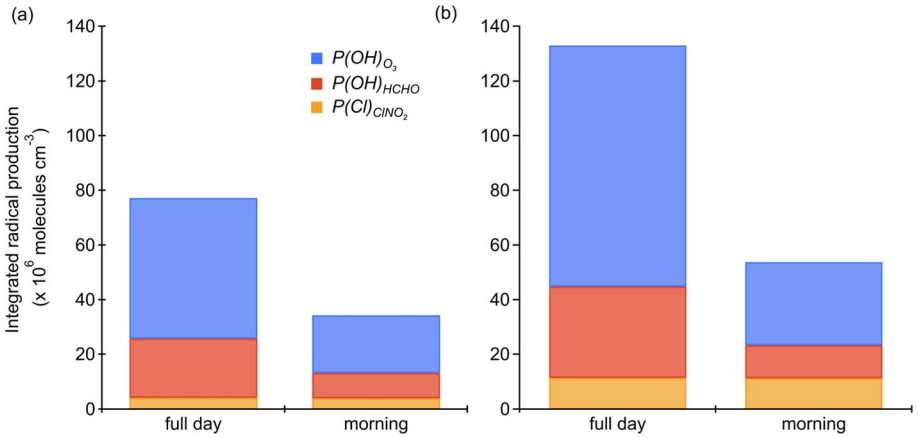

Fig. 5 Integrated ground-level radical production during the HaliFAQS campaign for three radical sources: $P(HO_x)$ from reaction of $O(^1D)$ from O_3 photolysis with water (blue), $P(HO_x)$ from diurnally averaged HCHO photolysis (red–orange), and P(Cl) from predicted $ClNO_2$ photolysis (yellow–orange) for (a) June 13 and (b) June 18 showing radical contributions for both the full day and the morning (06:00–12:00).

understanding of their relative contributions to initiating radical production and propagation.

3.3 Estimated influence of Cl_y as a primary radical source

We used the predicted Cl atoms formed from photolysis of $ClNO_2$ ($P(Cl)_{ClNO_2}$) for the two days with high irradiance and a single morning mode to assess the strength of this radical source compared to other major radical sources (Fig. 4 and 5). It should be noted that this is a radical source comparison and not a full radical budget, since we were unable to determine radical production from all of the primary radical sources (*e.g.*, HONO) that have been shown to be important in urban areas.[61–63] Due to this, the influence of Cl, as will be discussed below, should be interpreted as an upper limit as including these additional primary OH precursors would decrease Cl's contribution. Here, $P(Cl)_{ClNO_2}$ was determined from the lower, and therefore conservative, estimate of $[ClNO_2]_i$. As seen in Fig. 4, photolysis of O_3 (R11) and the subsequent reaction of $O(^1D)$ with water (R13) to yield OH ($P(HO_x)_{O_3}$) is the dominant radical producer during HaliFAQS, followed by photolysis of HCHO ((R14), $P(HO_x)_{HCHO}$), and finally $P(Cl)_{ClNO_2}$. Despite this, the contribution of Cl atoms to the morning radical population in Halifax is important relative to these other radical sources. The timing and impact are different because $P(HO_x)_{O_3}$ and $P(HO_x)_{HCHO}$ both peak near midday, while production of Cl from $ClNO_2$ peaks in mid-morning, around 10:00 am (Fig. 4). On June 13, $P(Cl)_{ClNO_2}$ was 8% of $P(HO_x)_{O_3}$ when considering the full day, and 19% when considering the 06:00–12:00 period of the morning (Fig. 5). On June 18, $P(Cl)_{ClNO_2}$ was 13% of $P(HO_x)_{O_3}$ when considering the full day, and 37% when considering the same morning period. Comparisons to other reports are limited, as only a few studies have calculated both $P(Cl)_{ClNO_2}$ and $P(HO_x)_{O_3}$. A radical budget from the CalNex campaign in Los Angeles during the summer of 2010 reported that $P(Cl)_{ClNO_2}$ was 11% of $P(HO_x)_{O_3}$ when averaged over eight sunny days and 37% in the same period of the mornings.[62] Radical production in Halifax on June 18 was lower in absolute terms for $P(HO_x)_{O_3}$ by approximately 45%, 90% lower for $P(HO_x)_{HCHO}$, and 50% lower for $P(Cl)_{ClNO_2}$.[62] Despite the maximum radical production being approximately half that observed in Los Angeles, the relative contributions of $P(Cl)_{ClNO_2}$ and $P(HO_x)_{O_3}$ are similar.

High levels of $ClNO_2$ in the morning will photolyze yielding Cl atoms that initiate oxidation and radical propagation earlier with respect to most OH radical sources. Another primary source of Cl atoms that has been shown to be important in polluted coastal areas is reaction between OH and HCl (R6).[7,8] We cannot estimate its importance during HaliFAQS, but it likely also contributed to the available Cl. In the NO_x-saturated O_3 regime that characterizes many urban areas including Halifax,[64] Cl atoms have a greater impact than OH on radical propagation and O_3 formation.[48]

4 Conclusions

In this work we made continuous, high time-resolution measurements of HCl in a coastal urban atmosphere during the HaliFAQS field campaign. Our inferred Cl activation chemistry and HCl levels are consistent with the limited observations in coastal locations around the world and these processes are likely present in any NO_x-polluted coastal areas. Bimodal peaks of HCl during days with high solar irradiance showed the presence of two photochemical production mechanisms. The first mode is consistent with the photolysis of Cl precursor compounds, and the second is most likely originating from HNO_3 acid displacement of HCl from chloride-containing aerosol.

We used the rate of change in measured HCl on 6 high irradiance mornings to calculate an equivalent Cl contribution from $ClNO_2$ as the most frequently observed and demonstrated precursor to HCl. The predicted HCl from the photolysis of the determined initial $ClNO_2$ showed good agreement for high irradiance days when using the 8:00 to 10:30 AM prediction period identified through our sensitivity analysis. Due to ongoing uncertainty around some HCl processes, we modeled the system with boundary conditions for the continual loss of HCl by deposition for low (1 cm s^{-1}) and high (6 cm s^{-1})

velocities, as well as conversion efficiencies of Cl to HCl of 77 and 100%, which is likely to encompass the conditions found in most urban environments. The resulting morning time trend and range of predicted HCl matched best for 1 cm s^{-1} and 77% CE, with agreement declining on days when a second afternoon HCl peak likely originating from HNO_3 chemistry was present, or when light levels were low. The higher deposition velocity models performed better in approximating the return to the initial baseline values. On June 18, the most photoactive day for Cl chemistry, it was possible to determine through a radical source comparison that $P(Cl)_{ClNO_2}$ contributed radicals at a relative abundance of 13% to $P(HO_x)_{O_3}$ across the entire day, increasing to 37% when considering the morning in isolation.

Photolabile Cl_y impacts air quality through both the early onset of radical formation and the differing reactivity of Cl atoms compared to OH radicals. In polluted coastal areas that are in a NO_x-saturated O_3 formation regime, Cl atoms have a greater impact on air quality than OH radicals.[48] Thus, it is important to include Cl in considerations of coastal urban air quality. To estimate the importance of Cl oxidation chemistry in the polluted marine boundary layer, we show here that high time resolution measurements of HCl could be used as an alternative to speciated Cl_y measurements, provided that future campaign intensives reach the same conclusion with full instrument suites capable of high time resolution speciated Cl_y, VOCs, speciated NO_y, size-resolved particulate and surface chloride measurements, and chemical models.

Author contributions

TCF and AM planned and conducted the fieldwork; quality controlled and finalized the collected datasets for HCl, NO_x, O_3, and irradiance; and conducted parts of the data analysis. CP and AW operated the OP-FTIR system and performed retrievals of HCHO concentrations from spectral measurements. TCF wrote the initial drafts of the manuscript. EMM conducted parts of the data analysis and wrote parts of the manuscript. CJY, TCV, RYWC, and AW conceptualized this study, and provided infrastructure and funding to carry it out. All authors participated in revisions to the writing of the manuscript.

Conflicts of interest

There are no conflicts to declare.

Note added after first publication

This version of the article is different to the Accepted Manuscript published on 7 January 2026. The Royal Society of Chemistry regrets that the Accepted Manuscript contained errors in the citations and reference list.

Data availability

The data supporting this article have been cited in the main text and are included as part of the supplementary information (SI). Supplementary information is available. See DOI: https://doi.org/10.1039/d5ea00115c.

The measurements in each dataset presented are also available through the Federated Research Data Repository of the Digital Research Alliance of Canada. See DOI: https://doi.org/10.20383/103.01566.

Acknowledgements

We acknowledge Natural Sciences Engineering and Research Council of Canada (NSERC) Discovery Grants (RGPIN-2018-05990, RGPIN-2020-06166), the Ocean Frontier Institute, and York University for funding. We thank Baban Nagare, and Joelle Dionne for assistance with data collection. EM was supported during this work by an Ontario Graduate Scholarship, Masters and Doctoral NSERC Canada Graduate Scholarships, the Charles Hantho graduate award in atmospheric chemistry at York University, and an Enbridge Graduate Student Award.

References

1 W. R. Simpson, S. S. Brown, A. Saiz-Lopez, J. A. Thornton and R. Von Glasow, Tropospheric Halogen Chemistry: Sources, Cycling, and Impacts, *Chem. Rev.*, 2015, **115**(10), 4035–4062, DOI: 10.1021/cr5006638.

2 A. Saiz-Lopez and R. von Glasow, Reactive Halogen Chemistry in the Troposphere, *Chem. Soc. Rev.*, 2012, **41**(19), 6448–6472, DOI: 10.1039/C2CS35208G.

3 G. Chen, Z. Chen, Y. Zhang, X. Fan, L. Xu, Z. Lin, X. Ji and J. Chen, Enhanced Oxidation Capacity Driven by Pollution-Induced Chlorine Chemistry in the Coastal Atmosphere, *npj Clim. Atmos. Sci.*, 2025, **8**(1), 248, DOI: 10.1038/s41612-025-01133-6.

4 W. Ma, X. Chen, M. Xia, Y. Liu, Y. Wang, Y. Zhang, F. Zheng, J. Zhan, C. Hua, Z. Wang, W. Wang, P. Fu, M. Kulmala and Y. Liu, Reactive Chlorine Species Advancing the Atmospheric Oxidation Capacities of Inland Urban Environments, *Environ. Sci. Technol.*, 2023, **57**(39), 14638–14647, DOI: 10.1021/acs.est.3c05169.

5 K. Kim, C. H. Song, K. M. Han, G. Yarwood, R. Beardsley and S. Kim, Incorporation of Multi-Phase Halogen Chemistry into the Community Multiscale Air Quality (CMAQ) Model, *Atmos. Chem. Phys.*, 2025, **25**(17), 10293–10314, DOI: 10.5194/acp-25-10293-2025.

6 W. Allan, H. Struthers and D. C. Lowe, Methane Carbon Isotope Effects Caused by Atomic Chlorine in the Marine Boundary Layer: Global Model Results Compared with Southern Hemisphere Measurements, *J. Geophys. Res. Atmos.*, 2007, **112**, 1–10, DOI: 10.1029/2006JD007369.

7 C. J. Young, R. A. Washenfelder, P. M. Edwards, D. D. Parrish, J. B. Gilman, W. C. Kuster, L. H. Mielke, H. D. Osthoff, C. Tsai, O. Pikelnaya, J. Stutz, P. R. Veres, J. M. Roberts, S. Griffith, S. Dusanter, P. S. Stevens, J. Flynn, N. Grossberg, B. Lefer, J. S. Holloway, J. Peischl, T. B. Ryerson, E. L. Atlas, D. R. Blake and S. S. Brown, Chlorine as a Primary Radical: Evaluation of Methods to Understand Its Role in Initiation of Oxidative Cycles,

Atmos. Chem. Phys., 2014, **14**, 3427–3440, DOI: 10.5194/acp-14-3427-2014.

8 T. P. Riedel, T. H. Bertram, T. A. Crisp, E. J. Williams, B. M. Lerner, A. Vlasenko, S.-M. Li, J. Gilman, J. de Gouw, D. M. Bon, N. L. Wagner, S. S. Brown and J. A. Thornton, Nitryl Chloride and Molecular Chlorine in the Coastal Marine Boundary Layer, *Environ. Sci. Technol.*, 2012, **46**, 10463–10470, DOI: 10.1021/es204632r.

9 C. Wang, J. Liggio, J. J. B. Wentzell, S. Jorga, A. Folkerson and J. P. D. Abbatt, Chloramines as an Important Photochemical Source of Chlorine Atoms in the Urban Atmosphere, *Proc. Natl. Acad. Sci. U. S. A.*, 2023, **120**(30), 1–8, DOI: 10.1073/pnas.2220889120.

10 M. M. J. W. van Herpen, Q. Li, A. Saiz-Lopez, J. B. Liisberg, T. Röckmann, C. A. Cuevas, R. P. Fernandez, J. E. Mak, N. M. Mahowald, P. Hess, D. Meidan, J.-B. W. Stuut and M. S. Johnson, Photocatalytic Chlorine Atom Production on Mineral Dust–Sea Spray Aerosols over the North Atlantic, *Proc. Natl. Acad. Sci. U. S. A.*, 2023, **120**(31), 1–8, DOI: 10.1073/pnas.2303974120.

11 M. Xia, Y. Jiang, J. Dai, Y. Liu, C. Yan, M. Kulmala and T. Wang, Chlorine Activation in Marine Air: Insights From Chemical Budgets of Molecular Chlorine and Hypochlorous Acid, *J. Geophys. Res.:Atmos.*, 2025, **130**(6), e2024JD042568, DOI: 10.1029/2024JD042568.

12 Y. Chen, M. Xia, J. Zhang, E. Tsiligiannis, C. Wu, C. Yan, R. Cai, G. Zheng, Y. Li, J. Guo, Z. An, Y. Li, X. Zhao, Q. Qu, C. Hua, Z. Wang, S. Wang, Y. Liu, L. Cao, K. He, M. Kulmala, M. Hallquist, T. Wang, D. Worsnop and J. Jiang, Chloramine Chemistry as a Missing Link in Atmospheric Chlorine Cycling, *Sci. Adv.*, 2025, **11**(44), eadv4298, DOI: 10.1126/sciadv.adv4298.

13 B. J. Finlayson-Pitts, M. J. Ezell and J. N. Pitts, Formation of Chemically Active Chlorine Compounds by Reactions of Atmospheric NaCl Particles with Gaseous N2O5 and ClONO2, *Nature*, 1989, **337**(6204), 241–244, DOI: 10.1038/337241a0.

14 J. M. Roberts, H. D. Osthoff, S. S. Brown, A. R. Ravishankara, D. Coffman, P. Quinn and T. Bates, Laboratory Studies of Products of N2O5 Uptake on Cl^- Containing Substrates, *Geophys. Res. Lett.*, 2009, **36**(20), L20808, DOI: 10.1029/2009GL040448.

15 Q. Li, L. Zhang, T. Wang, Y. J. Tham, R. Ahmadov, L. Xue, Q. Zhang and J. Zheng, Impacts of Heterogeneous Uptake of Dinitrogen Pentoxide and Chlorine Activation on Ozone and Reactive Nitrogen Partitioning: Improvement and Application of the WRF-Chem Model in Southern China, *Atmos. Chem. Phys.*, 2016, **16**(23), 14875–14890, DOI: 10.5194/acp-16-14875-2016.

16 G. Sarwar, H. Simon, J. Xing and R. Mathur, Importance of Tropospheric ClNO2 Chemistry across the Northern Hemisphere, *Geophys. Res. Lett.*, 2014, **41**(11), 4050–4058, DOI: 10.1002/2014GL059962.

17 J. M. Roberts, H. D. Osthoff, S. S. Brown and A. R. Ravishankara, N2O5 Oxidizes Chloride to Cl2 in Acidic Atmospheric Aerosol, *Science*, 2008, **321**(5892), 1059, DOI: 10.1126/science.1158777.

18 J. A. Thornton and J. P. D. Abbatt, N2O5 Reaction on Submicron Sea Salt Aerosol: Kinetics, Products, and the Effect of Surface Active Organics, *J. Phys. Chem. A*, 2005, **109**(44), 10004–10012, DOI: 10.1021/jp054183t.

19 H. Kim, R. J. Park, S. Kim, J. I. Jeong, D. Jeong, X. Fu and S. Cho, Effect of Nitryl Chloride Chemistry on Air Quality in South Korea during the KORUS-AQ Campaign, *Atmos. Environ.*, 2023, **312**, 120045, DOI: 10.1016/j.atmosenv.2023.120045.

20 T. D. Saul, M. P. Tolocka and M. V. Johnston, Reactive Uptake of Nitric Acid onto Sodium Chloride Aerosols Across a Wide Range of Relative Humidities, *J. Phys. Chem. A*, 2006, **110**(24), 7614–7620, DOI: 10.1021/jp060639a.

21 E. E. Gard, M. J. Kleeman, D. S. Gross, L. S. Hughes, J. O. Allen, B. D. Morrical, D. P. Fergenson, T. Dienes, M. E. Gälli, R. J. Johnson, G. R. Cass and K. A. Prather, Direct Observation of Heterogeneous Chemistry in the Atmosphere, *Science*, 1998, **279**(5354), 1184–1187, DOI: 10.1126/science.279.5354.1184.

22 A. Laskin, R. C. Moffet, M. K. Gilles, J. D. Fast, R. A. Zaveri, B. Wang, P. Nigge and J. Shutthanandan, Tropospheric Chemistry of Internally Mixed Sea Salt and Organic Particles: Surprising Reactivity of NaCl with Weak Organic Acids, *J. Geophys. Res.:Atmos.*, 2012, **117**(D15), D15302, DOI: 10.1029/2012JD017743.

23 S. Pechtl and R. von Glasow, Reactive Chlorine in the Marine Boundary Layer in the Outflow of Polluted Continental Air: A Model Study, *Geophys. Res. Lett.*, 2007, **34**(11), L11813, DOI: 10.1029/2007GL029761.

24 M. J. Rossi, Heterogeneous Reactions on Salts, *Chem. Rev.*, 2003, **103**(12), 4823–4882, DOI: 10.1021/cr020507n.

25 J. D. Raff, B. Njegic, W. L. Chang, M. S. Gordon, D. Dabdub, R. B. Gerber and B. J. Finlayson-Pitts, Chlorine Activation Indoors and Outdoors via Surface-Mediated Reactions of Nitrogen Oxides with Hydrogen Chloride, *Proc. Natl. Acad. Sci. U. S. A.*, 2009, **106**(33), 13647–13654, DOI: 10.1073/pnas.0904195106.

26 W. C. Keene, J. Stutz, A. A. P. Pszenny, J. R. Maben, E. V. Fischer, A. M. Smith, R. von Glasow, S. Pechtl, B. C. Sive and R. K. Varner, Inorganic Chlorine and Bromine in Coastal New England Air during Summer, *J. Geophys. Res.:Atmos.*, 2007, **112**(10), 1–15, DOI: 10.1029/2006JD007689.

27 W. C. Keene, M. A. K. Khalil, D. J. Erickson, A. McCulloch, T. E. Graedel, J. M. Lobert, M. L. Aucott, S. L. Gong, D. B. Harper, G. Kleiman, P. Midgley, R. M. Moore, C. Seuzaret, W. T. Sturges, C. M. Benkovitz, V. Koropalov, L. A. Barrie and Y. F. Li, Composite Global Emissions of Reactive Chlorine from Anthropogenic and Natural Sources: Reactive Chlorine Emissions Inventory, *J. Geophys. Res.*, 1999, **104**, 8429–8440.

28 M. Le Breton, A. Bacak, J. B. A. Muller, P. Xiao, B. M. A. Shallcross, R. Batt, M. C. Cooke, D. E. Shallcross, S. J. B. Bauguitte and C. J. Percival, Simultaneous Airborne Nitric Acid and Formic Acid Measurements Using a Chemical Ionization Mass Spectrometer around the UK: Analysis of Primary and Secondary Production Pathways,

Atmos. Environ., 2014, **83**(3), 166–175, DOI: 10.1016/j.atmosenv.2013.10.008.

29 H. Rodhe, P. Crutzen and A. Vanderpol, Formation of Sulfuric and Nitric Acid in the Atmosphere during Long-Range Transport, *Tellus*, 1981, **33**(2), 132–141, DOI: 10.1111/j.2153-3490.1981.tb01739.x.

30 A. H. Young, W. C. Keene, A. A. P. Pszenny, R. Sander, J. A. Thornton, T. P. Riedel and J. R. Maben, Phase Partitioning of Souble Trace Gases with Size-Resolved Aerosols in near-Surface Continental Air over Northern Colorado, USA, during Winter, *J. Geophys. Res.:Atmos.*, 2013, **118**, 9414–9427, DOI: 10.1002/jgrd.50655.

31 T. C. VandenBoer, C. J. Young, R. K. Talukdar, M. Z. Markovic, S. S. Brown, J. M. Roberts and J. G. Murphy, Nocturnal Loss and Daytime Source of Nitrous Acid through Reactive Uptake and Displacement, *Nat. Geosci.*, 2015, **8**(1), 55–60, DOI: 10.1038/ngeo2298.

32 A. A. Angelucci, T. C. Furlani, X. Wang, D. J. Jacob, T. C. Vandenboer and C. J. Young, Understanding Sources of Atmospheric Hydrogen Chloride in Coastal Spring and Continental Winter, *ACS Earth Space Chem.*, 2021, **5**(9), 2507–2516, DOI: 10.1021/acsearthspacechem.1c00193.

33 W. C. Keene, M. S. Long, A. A. P. Pszenny, R. Sander, J. R. Maben, A. J. Wall, T. L. O'Halloran, A. Kerkweg, E. V. Fischer and O. Schrems, Latitudinal Variation in the Multiphase Chemical Processing of Inorganic Halogens and Related Species over the Eastern North and South Atlantic Oceans, *Atmos. Chem. Phys.*, 2009, **9**(19), 7361–7385, DOI: 10.5194/acp-9-7361-2009.

34 T. A. Crisp, B. M. Lerner, E. J. Williams, P. K. Quinn, T. S. Bates and T. H. Bertram, Observations of Gas Phase Hydrochloric Acid in the Polluted Marine Boundary Layer, *J. Geophys. Res.*, 2014, 6897–6915, DOI: 10.1002/2013JD020992.

35 X. Wang, D. J. Jacob, S. D. Eastham, M. P. Sulprizio, L. Zhu, Q. Chen, B. Alexander, T. Sherwen, M. J. Evans, B. H. Lee, J. D. Haskins, F. D. Lopez-Hilfiker, J. A. Thornton, G. L. Huey and H. Liao, The Role of Chlorine in Global Tropospheric Chemistry, *Atmos. Chem. Phys.*, 2019, **19**(6), 3981–4003, DOI: 10.5194/acp-19-3981-2019.

36 J. W. Halfacre, J. Stewart, S. C. Herndon, J. R. Roscioli, C. Dyroff, T. I. Yacovitch, M. Flynn, S. J. Andrews, S. S. Brown, P. R. Veres and P. M. Edwards, Using Tunable Infrared Laser Direct Absorption Spectroscopy for Ambient Hydrogen Chloride Detection: HCl-TILDAS, *Atmos. Meas. Tech.*, 2023, **16**(5), 1407–1429, DOI: 10.5194/amt-16-1407-2023.

37 P. G. Eger, F. Helleis, G. Schuster, G. J. Phillips, J. Lelieveld and J. N. Crowley, Chemical Ionization Quadrupole Mass Spectrometer with an Electrical Discharge Ion Source for Atmospheric Trace Gas Measurement, *Atmos. Meas. Tech.*, 2019, **12**(3), 1935–1954, DOI: 10.5194/amt-12-1935-2019.

38 J. D. Haskins, L. Jaeglé, V. Shah, B. H. Lee, F. D. Lopez-Hilfiker, P. Campuzano-Jost, J. C. Schroder, D. A. Day, H. Guo, A. P. Sullivan, R. Weber, J. Dibb, T. Campos, J. L. Jimenez, S. S. Brown and J. A. Thornton, Wintertime Gas-Particle Partitioning and Speciation of Inorganic Chlorine in the Lower Troposphere Over the Northeast United States and Coastal Ocean, *J. Geophys. Res.:Atmos.*, 2018, **123**(22), 812–916, DOI: 10.1029/2018JD028786.

39 H. D. Osthoff, J. M. Roberts, A. R. Ravishankara, E. J. Williams, B. M. Lerner, R. Sommariva, T. S. Bates, D. Coffman, P. K. Quinn, J. E. Dibb, H. Stark, J. B. Burkholder, R. K. Talukdar, J. Meagher, F. C. Fehsenfeld and S. S. Brown, High Levels of Nitryl Chloride in the Polluted Subtropical Marine Boundary Layer, *Nat. Geosci.*, 2008, **1**(5), 324–328, DOI: 10.1038/ngeo177.

40 C. L. Hagen, B. C. Lee, I. S. Franka, J. L. Rath, T. C. Vandenboer, J. M. Roberts, S. S. Brown and A. P. Yalin, Cavity Ring-down Spectroscopy Sensor for Detection of Hydrogen Chloride, *Atmos. Meas. Tech.*, 2014, **7**(2), 345–357, DOI: 10.5194/amt-7-345-2014.

41 J. Wilkerson, D. Sayres, J. Smith, N. Allen, M. Rivero, M. Greenberg, T. Martin and J. Anderson, In Situ Observations of Stratospheric HCl Using Three-Mirror Integrated Cavity Output Spectroscopy, *Atmos. Meas. Tech.*, 2021, **14**(5), 3597–3613, DOI: 10.5194/amt-14-3597-2021.

42 T. C. Furlani, P. R. Veres, K. E. Dawe, J. A. Neuman, S. S. Brown, T. C. VandenBoer and C. J. Young, Validation of a New Cavity Ring-down Spectrometer for Measuring Tropospheric Gaseous Hydrogen Chloride, *Atmos. Meas. Tech.*, 2021, **14**(8), 5859–5871, DOI: 10.5194/amt-2021-105.

43 H. D. Osthoff, C. A. Odame-Ankrah, Y. M. Taha, T. W. Tokarek, C. L. Schiller, D. Haga, K. Jones and R. Vingarzan, Low Levels of Nitryl Chloride at Ground Level: Nocturnal Nitrogen Oxides in the Lower Fraser Valley of British Columbia, *Atmos. Chem. Phys.*, 2018, **18**(9), 6293–6315, DOI: 10.5194/acp-18-6293-2018.

44 R. McLaren, P. Wojtal, D. Majonis, J. McCourt, J. D. Halla and J. Brook, NO3 Radical Measurements in a Polluted Marine Environment: Links to Ozone Formation, *Atmos. Chem. Phys.*, 2010, **10**(9), 4187–4206, DOI: 10.5194/acp-10-4187-2010.

45 A. Wiacek, L. Li, K. Tobin and M. Mitchell, Characterization of Trace Gas Emissions at an Intermediate Port, *Atmos. Chem. Phys.*, 2018, **18**(19), 13787–13812, DOI: 10.5194/acp-18-13787-2018.

46 J. A. Milbrandt, S. Bélair, M. Faucher, M. Vallée, M. L. Carrera and A. Glazer, The Pan-Canadian High Resolution (2.5 Km) Deterministic Prediction System, *Weather Forecast.*, 2016, **31**(6), 1791–1816, DOI: 10.1175/WAF-D-16-0035.1.

47 S. Madronich, and S. Flocke, The Role of Solar Radiation in Atmospheric Chemistry, in *Handbook of Environmental Chemistry*, ed. P. Boule, Springer-Verlag, Heidelberg, 1998, pp. 1–26.

48 P. M. Edwards and C. J. Young, Primary Radical Effectiveness: Do the Different Chemical Reactivities of Hydroxyl and Chlorine Radicals Matter for Tropospheric Oxidation?, *ACS ES&T Air*, 2024, **1**(8), 780–788, DOI: 10.1021/acsestair.3c00108.

49 B. K. Place, C. J. Young, S. E. Ziegler, K. A. Edwards, L. Salehpoor and T. C. VandenBoer, Passive Sampling

Capabilities for Ultra-Trace Quantitation of Atmospheric Nitric Acid (HNO3) in Remote Environments, *Atmos. Environ.*, 2018, **191**, 360–369, DOI: 10.1016/j.atmosenv.2018.08.030.

50 B. J. Finlayson-Pitts, and J. N. Pitts Jr, *Chemistry of the Upper and Lower Atmosphere: Theory, Experiments, and Applications*, Academic Press, San Diego, CA, 2000.

51 Y. Zhang, W. Ma and L. Chen, Influence of Rough Flow over Sea Surface on Dry Atmospheric Deposition Velocities, *Terr. Atmos. Ocean Sci.*, 2013, **24**(5), 877, DOI: 10.3319/TAO.2013.05.09.01(A).

52 A. B. Meinel, and M. P. Meinel, *Applied Solar Energy Addison*, Wesley Publishing Co, 1976.

53 H. Woolf, *On the Computation of Solar Elevation Angles and the Determination of Sunrise and Sunset Times*, 1968.

54 F. Kasten and A. T. Young, Revised Optical Air Mass Tables and Approximation Formula, *Appl. Opt.*, 1989, **28**(22), 4735–4738, DOI: 10.1364/AO.28.004735.

55 C. J. Young, R. A. Washenfelder, J. M. Roberts, L. H. Mielke, H. D. Osthoff, C. Tsai, O. Pikelnaya, J. Stutz, P. R. Veres, A. K. Cochran, T. C. Vandenboer, J. Flynn, N. Grossberg, C. L. Haman, B. Lefer, H. Stark, M. Graus, J. De Gouw, J. B. Gilman, W. C. Kuster and S. S. Brown, Vertically Resolved Measurements of Nighttime Radical Reservoirs in Los Angeles and Their Contribution to the Urban Radical Budget, *Environ. Sci. Technol.*, 2012, **46**(20), 10965–10973, DOI: 10.1021/es302206a.

56 J. D. Haskins, L. Jaeglé, V. Shah, B. H. Lee, F. D. Lopez-Hilfiker, P. Campuzano-Jost, J. C. Schroder, D. A. Day, H. Guo, A. P. Sullivan, R. Weber, J. Dibb, T. Campos, J. L. Jimenez, S. S. Brown and J. A. Thornton, Wintertime Gas-Particle Partitioning and Speciation of Inorganic Chlorine in the Lower Troposphere over the Northeast United States and Coastal Ocean, *J. Geophys. Res.:Atmos.*, 2018, **123**(22), 897–916, DOI: 10.1029/2018JD028786.

57 Y. Tao, T. C. VandenBoer, P. R. Veres, C. Warneke, J. A. de Gouw, R. J. Weber, M. Z. Markovic, Y. Zhao, K. R. Baker, J. T. Kelly, J. G. Murphy, C. J. Young and J. M. Roberts, Hydrogen Chloride (HCl) at Ground Sites During CalNex 2010 and Insight Into Its Thermodynamic Properties, *J. Geophys. Res.:Atmos.*, 2022, **127**(9), e2021JD036062, DOI: 10.1029/2021JD036062.

58 M. J. Lawler, B. D. Finley, W. C. Keene, A. A. P. Pszenny, K. A. Read, R. von Glasow and E. S. Saltzman, Pollution-Enhanced Reactive Chlorine Chemistry in the Eastern Tropical Atlantic Boundary Layer, *Geophys. Res. Lett.*, 2009, **36**(8), L08810, DOI: 10.1029/2008GL036666.

59 B. Jourdain and M. Legrand, Year-Round Records of Bulk and Size-Segregated Aerosol Composition and HCl and HNO3 Levels in the Dumont d'Urville (Coastal Antarctica) Atmosphere: Implications for Sea-Salt Aerosol Fractionation in the Winter and Summer, *J. Geophys. Res.:Atmos.*, 2002, **107**(D22), 1–13, DOI: 10.1029/2002JD002471.

60 W. C. Keene, A. A. P. Pszenny, J. R. Maben, E. Stevenson and A. Wall, Closure Evaluation of Size-Resolved Aerosol PH in the New England Coastal Atmosphere during Summer, *J. Geophys. Res.:Atmos.*, 2004, **109**(D23), D23307, DOI: 10.1029/2004JD004801.

61 S. Kim, T. C. VandenBoer, C. J. Young, T. P. Riedel, J. A. Thornton, B. Swarthout, B. Sive, B. Lerner, J. B. Gilman, C. Warneke, J. M. Roberts, A. Guenther, N. L. Wagner, W. P. Dubé, E. Williams and S. S. Brown, The Primary and Recycling Sources of OH during the NACHTT-2011 Campaign: HONO as an Important OH Primary Source in the Wintertime, *J. Geophys. Res.:Atmos.*, 2014, **119**(11), 6886–6896, DOI: 10.1002/2013JD019784.

62 C. J. Young, R. A. Washenfelder, J. M. Roberts, L. H. Mielke, H. D. Osthoff, C. Tsai, O. Pikelnaya, J. Stutz, P. R. Veres, A. K. Cochran, T. C. VandenBoer, J. Flynn, N. Grossberg, C. L. Haman, B. Lefer, H. Stark, M. Graus, J. de Gouw, J. B. Gilman, W. C. Kuster and S. S. Brown, Vertically Resolved Measurements of Nighttime Radical Reservoirs in Los Angeles and Their Contribution to the Urban Radical Budget, *Environ. Sci. Technol.*, 2012, **46**(20), 10965–10973, DOI: 10.1021/es302206a.

63 B. Alicke, U. Platt and J. Stutz, Impact of Nitrous Acid Photolysis on the Total Hydroxyl Radical Budget during the Limitation of Oxidant Production/Pianura Padana Produzione Di Ozono Study in Milan, *J. Geophys. Res.:Atmos.*, 2002, **107**(D22), 1–17, DOI: 10.1029/2000JD000075.

64 M. Mitchell, A. Wiacek and I. Ashpole, Surface Ozone in the North American Pollution Outflow Region of Nova Scotia: Long-Term Analysis of Surface Concentrations, Precursor Emissions and Long-Range Transport Influence, *Atmos. Environ.*, 2021, **261**, 118536, DOI: 10.1016/j.atmosenv.2021.118536.